AIP | Physics of Plasmas

A simple ideal magnetohydrodynamical model of vertical disruption events in tokamaks

R. Fitzpatrick

Citation: Physics of Plasmas (1994-present) **16**, 012506 (2009); doi: 10.1063/1.3068467
View online: http://dx.doi.org/10.1063/1.3068467
View Table of Contents: http://scitation.aip.org/content/aip/journal/pop/16/1?ver=pdfcov
Published by the AIP Publishing

A simple ideal magnetohydrodynamical model of vertical disruption events in tokamaks

R. Fitzpatrick
Institute for Fusion Studies, Department of Physics, University of Texas at Austin, Austin, Texas 78712, USA

(Received 7 August 2008; accepted 18 December 2008; published online 27 January 2009)

A simple model of axisymmetric vertical disruption events (VDEs) in tokamaks is presented in which the halo current force exerted on the vacuum vessel is calculated directly from linear, marginally stable, ideal-magnetohydrodynamical (MHD) stability analysis. The basic premise of the model is that the halo current force modifies pressure balance at the edge of the plasma, and therefore also modifies ideal-MHD plasma stability. In order to prevent the ideal vertical instability, responsible for the VDE, from growing on the very short Alfvén time scale, the halo current force must adjust itself such that the instability is rendered marginally stable. The model predicts halo currents which are similar in magnitude to those observed experimentally. An approximate nonaxisymmetric version of the model is developed in order to calculate the toroidal peaking factor for the halo current force. © *2009 American Institute of Physics*. [DOI: 10.1063/1.3068467]

I. INTRODUCTION

Tokamak plasma discharges are occasionally terminated by sudden events, known as *disruptions*, in which the plasma thermal energy and electric current are both rapidly quenched.[1] Elongated plasmas often become vertically unstable during disruptions, leading to so-called *vertical displacement events* (VDEs) in which the plasma makes contact with the vacuum vessel. When this happens, part of the plasma current, known as the *halo current*, flows through the vessel, producing a strong outward force.[2] Indeed, halo currents typically give rise to the largest forces experienced by the vacuum vessel during the lifetime of a tokamak. Consequently, halo current forces are a critical issue for the design and operation of ITER.[3–5]

In this paper, we present a relatively simple model of VDEs in tokamaks. The model employs a suitably modified version of conventional, marginally stable, *ideal-MHD* (magnetohydrodynamical) stability analysis to directly determine the size of the halo current force. Since our aim is to calculate the maximum possible value of this force, we have examined a worst case scenario in which the plasma thermal quench does not occur prior to the onset of the vertical instability (i.e., a so-called "hot plasma" VDE).[6] Furthermore, for the sake of simplicity, all of the calculations described in this paper are performed using large aspect-ratio *sharp boundary* plasma equilibria.[7,8]

One important effect which is absent from our model is *wall eddy currents*. In practice, wall eddy currents are essential for maintaining vertical position control of elongated tokamak plasmas, since, without them, vertical instabilities would grow too rapidly to be controlled by any realistic feedback system.[9] Wall eddy currents are neglected in our model both to elucidate the role of halo currents in moderating vertical instabilities, and for the sake of simplicity. Of course, a realistic VDE model must incorporate both wall eddy currents and halo currents.

II. ORTHOGONAL CURVILINEAR COORDINATES

Consider a large aspect-ratio, axisymmetric, tokamak plasma equilibrium of major radius R. Suppose that the poloidal cross section of the plasma boundary is a *vertically elongated ellipse*. Let x and z be horizontal and vertical Cartesian coordinates, respectively, in the poloidal plane, which are defined such that the geometric center of the plasma lies at $x=z=0$. Adopting standard elliptical coordinates, we can write

$$x = as\sqrt{\kappa^2 - 1}\,\sinh\mu\cos\nu, \tag{1}$$

$$z = as\sqrt{\kappa^2 - 1}\,\cosh\mu\sin\nu, \tag{2}$$

where a is the initial plasma minor radius, s a dimensionless scale-factor, and $\kappa \geqslant 1$. Here, $\mu(x,z)$ is a label for a set of nested axisymmetric toroidal surfaces whose poloidal cross sections are vertically elongated ellipses, and $\nu(x,z)$ is an anglelike poloidal coordinate. The innermost (zero volume) surface corresponds to $\mu=0$, whereas the outermost (infinite volume) surface corresponds to $\mu=\infty$. Note that $\nabla\mu\cdot\nabla\nu=0$ everywhere in the poloidal plane. It is easily demonstrated that $|\nabla\mu|=|\nabla\nu|=(ah)^{-1}$, where $h(\mu,\nu)=s\sqrt{\kappa^2-1}[\sinh^2\mu+\cos^2\nu]^{1/2}$. Moreover, if ϕ is the toroidal angle, then $|\nabla\phi|=R^{-1}$, assuming that $\epsilon\equiv a/R\ll 1$. A general vector can be written $\mathbf{A}=A_\mu\mathbf{e}_\mu+A_\nu\mathbf{e}_\nu+A_\phi\mathbf{e}_\phi$, where $\mathbf{e}_\mu=\nabla\mu/|\nabla\mu|$, etc. In the following, μ, ν, ϕ are employed as a set of orthogonal curvilinear coordinates.

III. SHARP BOUNDARY PLASMA EQUILIBRIA

Let the plasma boundary coincide with the toroidal surface $\mu=\mu_a$, where $\mu_a=\tanh^{-1}(\kappa^{-1})$. This implies that, in the poloidal plane, the plasma is bounded by the vertically elongated ellipse $x=a\,s\cos\nu$, $z=\kappa\,a\,s\sin\nu$. It follows that $a\,s$ is the minor radius of the plasma, and κ its vertical elongation.

Consider a so-called *sharp-boundary* plasma equilibrium which is *current-free* with *constant pressure*, P.[7] The equi-

librium toroidal magnetic field-strengths inside and outside the plasma are written as $B_i/(1+x/R)$ and $B_o/(1+x/R)$, respectively, where B_i and B_o are constants. There is no poloidal magnetic field within the plasma. However, a poloidal field is generated outside the plasma by a *current sheet* flowing on the plasma boundary. Let the components of this external poloidal field at the edge of the plasma be $B_\mu=0$ and $B_\nu=B_\nu(\nu)$.

Pressure balance across the plasma boundary yields[7]

$$P+\frac{1}{2\mu_0}\left(\frac{B_i}{1+\epsilon s\cos\nu}\right)^2=\frac{1}{2\mu_0}\left[\left(\frac{B_o}{1+\epsilon s\cos\nu}\right)^2+B_\nu^2\right]. \tag{3}$$

It is convenient to adopt the following large aspect-ratio, high-β (i.e., $\beta\sim\epsilon$, rather than $\beta\sim\epsilon^2$) orderings:[7] $\epsilon\ll 1$, $\beta\sim\epsilon$, $(B_o-B_i)/B_o\sim\epsilon$, and $\beta+B_i^2/B_o^2-1\sim\epsilon^2$. Here, $\beta=2\mu_0 P/B_o^2$. Making use of the above orderings, Eq. (3) reduces to[7]

$$\hat{B}_\nu(\nu)=[A+2\hat{\beta}s\cos\nu]^{1/2}, \tag{4}$$

where A is an $O(1)$ constant, $\hat{B}_\nu=B_\nu/(\epsilon B_o)$, and $\hat{\beta}=\beta/\epsilon$. Now, the safety-factor at the plasma boundary is defined as[7]

$$q_a=\oint\frac{h_a(\nu)}{\hat{B}_\nu(\nu)}\frac{d\nu}{2\pi}, \tag{5}$$

where

$$h_a(\nu)\equiv h(\mu_a,\nu)=s[1+(\kappa^2-1)\cos^2\nu]^{1/2}. \tag{6}$$

Writing $A=2\hat{\beta}s(2/\alpha^2-1)$, we obtain

$$\alpha Q(\alpha)=\pi q_a\hat{\beta}^{1/2}s^{1/2}, \tag{7}$$

with

$$Q(\alpha)=\frac{1}{2}\int_0^\pi\frac{h_a(\nu)d\nu}{[1-\alpha^2\sin^2(\nu/2)]^{1/2}}. \tag{8}$$

Let $\mathbf{i}_p$ be the equilibrium current sheet density (i.e., radially integrated current density) flowing on the plasma boundary. It is easily demonstrated that

$$\mu_0 i_{p\nu}=-\tfrac{1}{2}\beta B_o, \tag{9}$$

$$\mu_0 i_{p\phi}=B_\nu. \tag{10}$$

Thus, the electromagnetic pressure exerted on the plasma boundary due to the current sheet is

$$P_p=\mathbf{e}_\mu\cdot\mathbf{i}_p\times\mathbf{B}\simeq-\frac{1}{2\mu_0}\beta B_o^2=-P. \tag{11}$$

Clearly, the electromagnetic pressure at the boundary acts inward, and is exactly balanced by the outward acting plasma pressure.

Throughout this paper, current is normalized as $\hat{I}=\mu_0 I/(a\epsilon B_o)$. Hence, the normalized components of the net equilibrium plasma current are

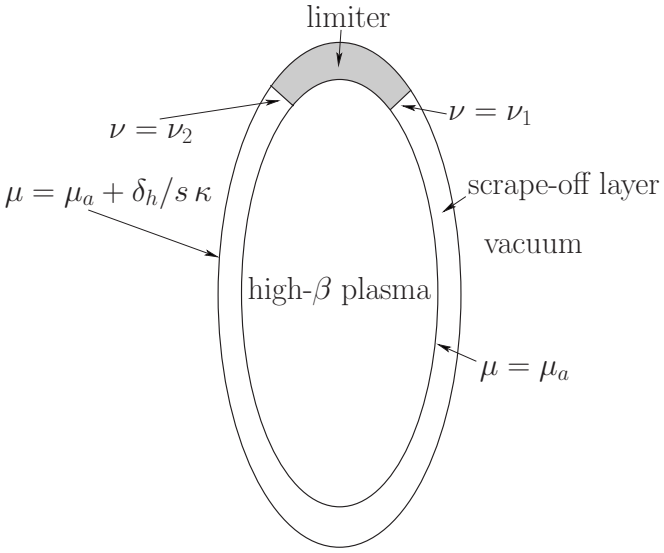

FIG. 1. Schematic diagram showing the poloidal cross section of a high-β plasma surrounded by an axisymmetric halo consisting of a low-β scrape-off layer and a rigid conducting limiter.

$$\hat{I}_{p\nu}=-\epsilon^{-1}\pi\hat{\beta}, \tag{12}$$

$$\hat{I}_{p\phi}=\oint h_a(\nu)\hat{B}_\nu(\nu)d\nu. \tag{13}$$

IV. AXISYMMETRIC HALO CURRENTS

Suppose that the edge of the above-mentioned plasma equilibrium is in contact with an axisymmetric rigid conductor, which is termed the *limiter*, and which extends over the range of poloidal angles $\nu_1<\nu<\nu_2$. For the sake of simplicity, let the limiter lie between the toroidal surfaces $\mu=\mu_a$ and $\mu=\mu_a+\delta_h/(s\kappa)$. The scrape-off layer (SOL) is a low-β plasma which is also situated between the toroidal surfaces $\mu=\mu_a$ and $\mu=\mu_a+\delta_h/(s\kappa)$, and extends over all poloidal angles except those in the range $\nu_1<\nu<\nu_2$. The maximum radial width of the SOL is $a\delta_h$. It is assumed that $\delta_h\ll 1$. All magnetic flux-surfaces lying within the SOL intersect the limiter. The limiter and SOL are collectively known as the *halo*. The halo is sandwiched between a high-β plasma (with closed flux-surfaces) on the inside (i.e., the region $\mu<\mu_a$), and a vacuum on the outside [i.e., the region $\mu>\mu_a+\delta_h/(s\kappa)$], see Fig. 1. In the following, any μ-variation within the halo is neglected, for the sake of simplicity. Incidentally, the "limiter" in our analysis might represent a real limiter, a divertor, or even a section of the vacuum vessel.

Any current flowing within the halo is termed a *halo current*. In general, there is no halo current associated with the unperturbed plasma equilibrium. Suppose, however, that the plasma is forced to move toward the limiter by an ideal vertical (i.e., $n=0$, where n is the toroidal mode number) instability. We would expect this movement to cause the plasma's outermost magnetic flux-surfaces to intersect the limiter, and to also generate a halo current flowing around these surfaces.[10]

Now, given that the SOL plasma is low-β (since it is relatively cold, due to rapid parallel heat transport to the limiter) any currents flowing in it must be approximately "force-free" (i.e., they must flow parallel to equilibrium magnetic field lines).[11] Thus, the halo current sheet density, $\mathbf{i}_h$, has the components

$$i_{h\nu} = \frac{P_0}{B_o}, \tag{14}$$

$$i_{h\phi} = \frac{P_0}{B_\nu}, \tag{15}$$

in the SOL, where P_0 is a constant. Here, we have made the reasonable assumption that the poloidal component of the halo current sheet density associated with an $n=0$ vertical instability is *axisymmetric*. Of course, there is no constraint that the halo current be force-free in the limiter, since any associated electromagnetic force can be balanced there by mechanical stresses.[8] Thus, we would expect the halo current to flow across the limiter along the shortest path (i.e., the path of least electrical resistance). For the case of a large aspect-ratio tokamak, and an axisymmetric limiter which only extends over a relatively small range of poloidal angles, the shortest path is almost purely poloidal. It follows that in the limiter the halo current flows in the poloidal direction. In other words,

$$i_{h\nu} = \frac{P_0}{B_o}, \tag{16}$$

$$i_{h\phi} = 0, \tag{17}$$

in the limiter. Note that the poloidal component of the halo current sheet density must be *continuous* across the SOL/limiter boundary, in order to conserve charge, whereas the toroidal component is allowed to be discontinuous.

The halo current induced electromagnetic pressure acting on the SOL is zero, by definition. On the other hand, the electromagnetic pressure acting on the limiter is

$$P_h = \mathbf{e}_\mu \cdot \mathbf{i}_h \times \mathbf{B} = P_0. \tag{18}$$

Note that this pressure is *axisymmetric*.

As is easily demonstrated, the components of the normalized net halo current are

$$\hat{I}_{h\nu} = 2\pi \hat{P}_0, \tag{19}$$

$$\hat{I}_{h\phi} = (1-\alpha_h) q_a \hat{I}_{h\nu}, \tag{20}$$

where $\hat{P}_0 = \mu_0 P_0/(\epsilon B_o)^2$, and

$$\alpha_h = \int_{\nu_1}^{\nu_2} h_a d\nu/\hat{B}_\nu \Big/ \oint h_a d\nu/\hat{B}_\nu. \tag{21}$$

Assuming that $\hat{\beta}$ and $\hat{P}_0$ are $O(1)$, it is clear, from Eqs. (12) and (19), that the poloidal halo current is always *much less* than the poloidal plasma current.

V. IDEAL PLASMA STABILITY

Consider a marginally stable, ideal plasma instability. Assuming that the perturbed current is zero inside the plasma, it follows that the perturbed pressure is also zero. Hence, we can write the perturbed magnetic fields both inside and outside the plasma in the form $\delta\mathbf{B} = i\nabla V$, where $\nabla^2 V = 0$.

According to Ref. 12, the perturbed matching conditions at the plasma boundary, $\mu = \mu_a$, are

$$[\mathbf{e}_\mu \cdot \delta\mathbf{B} - \mathbf{B}\cdot\nabla\xi + \xi \mathbf{e}_\mu \cdot (\mathbf{e}_\mu \cdot \nabla)\mathbf{B}]_i = 0, \tag{22}$$

$$[\mathbf{e}_\mu \cdot \delta\mathbf{B} - \mathbf{B}\cdot\nabla\xi + \xi \mathbf{e}_\mu \cdot (\mathbf{e}_\mu \cdot \nabla)\mathbf{B}]_o = 0, \tag{23}$$

$$\mu_0^{-1}[\mathbf{B}\cdot\delta\mathbf{B} + \xi \mathbf{e}_\mu \cdot \nabla(B^2/2)]_i = \mu_0^{-1}[\mathbf{B}\cdot\delta\mathbf{B} + \xi \mathbf{e}_\mu \cdot \nabla(B^2/2)]_o, \tag{24}$$

where the subscripts i and o refer to inside and outside the boundary, respectively, and $\xi(\nu,\phi)$ is the edge plasma displacement. The first two matching conditions ensure that the boundary remains a magnetic flux-surface, whereas the final matching condition enforces pressure balance. Of course, the limiter force associated with an axisymmetric halo current affects pressure balance at the plasma boundary. In the presence of such a force, it seems plausible to modify Eq. (24) as follows:[13]

$$\mu_0^{-1}[\mathbf{B}\cdot\delta\mathbf{B} + \xi \mathbf{e}_\mu \cdot \nabla(B^2/2)]_i = \mu_0^{-1}[\mathbf{B}\cdot\delta\mathbf{B} + \xi \mathbf{e}_\mu \cdot \nabla(B^2/2)]_o + f_0 \zeta \xi, \tag{25}$$

where $f_0 = P_0/(a\delta_h h_a/s\kappa)$ is the normal component of the *limiter force density*. Here, $\zeta = 1$ for $\nu_1 < \nu < \nu_2$, and $\zeta = 0$, otherwise. The additional term on the right-hand side of the above equation represents the virtual work done on the displaced plasma by the reaction to the limiter force.

Following the analysis of Ref. 8, the matching conditions at the plasma boundary, $\mu = \mu_a$, reduce to

$$\mathrm{i}\frac{\partial \hat{V}_i}{\partial \mu} = h_a \frac{\partial \hat{\xi}}{\partial \phi}, \tag{26}$$

$$\mathrm{i}\frac{\partial \hat{V}_o}{\partial \mu} = \left(\hat{B}_\nu \frac{\partial}{\partial \nu} + h_a \frac{\partial}{\partial \phi}\right)\hat{\xi} + \frac{\partial \hat{B}_\nu}{\partial \nu}\hat{\xi}, \tag{27}$$

$$\mathrm{i}\left(\hat{B}_\nu \frac{\partial}{\partial \nu} + h_a \frac{\partial}{\partial \phi}\right)\hat{V}_o - \mathrm{i}h_a \frac{\partial \hat{V}_i}{\partial \phi} = s\kappa\left(\frac{s\hat{B}_\nu^2}{h_a^2} + \hat{\beta}\cos\nu - \frac{\hat{P}_0 \zeta}{\delta_h h_a}\right)\hat{\xi}, \tag{28}$$

where $\hat{V}_{i,o} = V_{i,o}/(a\epsilon B_o)$, and $\hat{\xi} = \xi/a$. The potentials $\hat{V}_i$ and $\hat{V}_o$ both satisfy

$$\nabla^2 \hat{V}_{i,o} \simeq \frac{\partial^2 \hat{V}_{i,o}}{\partial^2 \mu} + \frac{\partial^2 \hat{V}_{i,o}}{\partial^2 \nu} = 0. \tag{29}$$

Suppose that all perturbed quantities vary toroidally as $\exp(-in\phi)$, where n is the toroidal mode number. The most general solution of Eq. (29) which is well behaved as $\mu\rightarrow 0$ is[8]

$$\hat{V}_i(\mu,\nu,\phi)=\sum_m \{a_m \cosh(m\mu)\cos[m(\nu-\pi/2)] + b_m \sinh(m\mu)\sin[m(\nu-\pi/2)]\}e^{-in\phi}, \quad (30)$$

where the a_m and b_m are constants. Likewise, in the absence of external conductors, the most general solution of Eq. (29) which is well-behaved as $\mu\rightarrow\infty$ is

$$\hat{V}_o(\mu,\nu,\phi)=\sum_m \hat{a}_m e^{-|m|(\mu-\mu_a)}e^{i(m\nu-n\phi)}, \quad (31)$$

where the $\hat{a}_m$ are constants.

Let $\xi(\nu,\phi)=\Sigma\xi_m e^{i(m\nu-n\phi)}$, where the ξ_m are constants. Following the analysis of Ref. 8, Eqs. (30) and (31), and the three matching conditions (26)–(28), reduce to the homogenous matrix equation $\Sigma_{m'}F_{mm'}\xi_{m'}=0$, which must be solved subject to the incompressibility constraint $\Sigma_{m'}G_{0m'}\xi_{m'}=0$. Here,

$$F_{mm'}=\sum_{k\neq 0} G_{km}|k|^{-1}\left[\frac{1+\iota^{2|k|}}{1-\iota^{2|k|}}G_{km'}+\frac{2(-\iota)^{|k|}}{1-\iota^{2|k|}}G_{-km'}\right] + \sum_{k\neq 0}\hat{G}_{km}|k|^{-1}\hat{G}_{km'}-H_{mm'}, \quad (32)$$

and

$$G_{mm'}=\oint [-nh_a(\nu)]e^{i(m'-m)\nu}\frac{d\nu}{2\pi}, \quad (33)$$

$$\hat{G}_{mm'}=\oint [m\hat{B}_\nu(\nu)-nh_a(\nu)]e^{i(m'-m)\nu}\frac{d\nu}{2\pi}, \quad (34)$$

$$H_{mm'}=s\kappa\oint\left(\frac{s\hat{B}_\nu^2}{h_a^2}+\hat{\beta}\cos\nu-\frac{P_0\zeta}{\delta_h h_a}\right)e^{i(m'-m)\nu}\frac{d\nu}{2\pi}, \quad (35)$$

with $\iota=(\kappa-1)/(\kappa+1)$.

The stability problem essentially reduces to the solution of the eigenmode equation

$$\sum_{m'} F_{mm'}\xi_{m'}=\lambda\xi_m, \quad (36)$$

subject to the constraint

$$\sum_{m'} G_{0m'}\xi_{m'}=0. \quad (37)$$

(Of course, only the $\lambda=0$ solution, which corresponds to the marginal stable case, is physical.) This is equivalent to solving the unconstrained eigenmode equation[7]

$$\sum_{m'}\tilde{F}_{mm'}z_{m'}=\lambda z_m, \quad (38)$$

where $\tilde{F}_{mm'}=\Sigma_{k,l}P_{mk}F_{kl}P_{lm'}$, and

$$P_{mm'}=\delta_{mm'}-\frac{G_{0m}G_{0m'}}{\Sigma_k G_{0k}^2}, \quad (39)$$

with $\xi_m=\Sigma_{m'}P_{mm'}z_{m'}$. Note that the $\tilde{F}_{mm'}$ matrix is real and symmetric, which guarantees that all of its eigenvalues are *real*. According to the ideal energy principle, the plasma is ideally *unstable* if any of the eigenvalues of Eq. (38) are *negative*, and stable otherwise.[12]

The $n=0$ mode is a special case, since the constraint (37) is automatically satisfied, due to the fact that the $G_{0m'}$ are all zero. In this situation, the plasma perturbation can be made incompressible by simply setting $\xi_0=0$. Hence, the eigenmode equation for the $n=0$ mode is

$$\sum_{m'\neq 0} F_{mm'}\xi_{m'}=\lambda\xi_m \quad (40)$$

for $m\neq 0$.

VI. AN IDEAL-MHD MODEL OF AXISYMMETRIC VDEs

A vertical disruption event (VDE) occurs when an elongated tokamak plasma equilibrium is subject to an ideal $n=0$ instability which causes it to move vertically toward a rigid conductor situated either above or below it. This conductor is termed the "limiter." For the sake of argument, let the limiter lie above the plasma. Thus, the upward movement of the plasma causes its outermost flux-surfaces to intersect the limiter, and also induces a halo current which flows around the intersected surfaces. As we have seen, the halo current is force-free in the scrape-off layer (i.e., the plasma-filled segment of the intersected flux-surfaces), but flows across equilibrium magnetic field lines in the limiter. Thus, the halo current gives rise to a net electromagnetic force acting on the limiter. It turns out that this force is always *outward*.

In general, an ideal $n=0$ plasma instability (which is not effectively moderated by eddy currents flowing in external conductors) grows on an *Alfvén time scale* (which is typically 10^{-7} s in a modern tokamak).[12] However, as soon as the plasma intersects the limiter, and a halo current flows across it, the associated force modifies pressure balance at the plasma boundary, and is, thereby, able to moderate the growth of the instability.[13] (This moderating effect is represented by the parameter $\hat{P}_0$ in the stability analysis of the previous section.) In general, we would expect the instability to be slowed down to such an extent that it grows on a typical *resistive time scale* calculated using the electrical resistance of the SOL plasma and the limiter, see Sec. VIII.[14] Such a time scale is inevitably *very much longer* than an Alfvén time. (In fact, a typical SOL/limiter resistive time scale in a modern tokamak is about 10^{-3} s.[14]) Hence, the moderating effect of the limiter force effectively renders the plasma *marginally stable* to the ideal $n=0$ mode. This crucial insight, due to Zakharov,[13] allows us to construct a linear *ideal-MHD* model of a vertical disruption event.

To be more exact, the $n=0$ force-matrix, $F_{mm'}$, of a plasma which is ideally unstable to the $n=0$ mode possesses one negative eigenvalue. In order to prevent the $n=0$ mode

from growing on the very short Alfvén time scale, the value of limiter force parameter, $\hat{P}_0$, must be adjusted such that this eigenvalue is set to *zero* (i.e., such that the mode is rendered marginally stable). We always find that the required value of $\hat{P}_0$ is *positive*, which corresponds to an *outward* force acting on the limiter. Note that as long as the SOL/limiter resistive time scale remains much longer than the Alfvén time scale, the limiter force parameter is solely determined by linear *ideal-MHD*. In particular, the force parameter is *independent* of the SOL/limiter resistive time scale. The same is also true for an $n=0$ mode moderated by eddy currents flowing in external conductors, provided that the slowed down instability grows on a time scale which is significantly shorter than the SOL/limiter resistive time scale. In the opposite case, the halo current is likely to be largely suppressed.

Now, we can crudely simulate the sequence of plasma equilibria during a VDE by gradually decreasing the scale factor s from unity, thereby causing a proportional decrease in the poloidal dimensions of the plasma. (Recall that the minor radius of the plasma is $a\,s$.) This sequence of equilibria is generated as the high-β plasma moves vertically, and consequently shrinks in size, because an increasing fraction of its flux-surfaces are intersected by the limiter, and so become part of the low-β halo. Since the motion of the plasma takes place on a much longer time scale than the Alfvén time scale, we can safely assume that the plasma is always close to an equilibrium state. Obviously, we must imagine that our equilibria move upward, as they shrink in size, so that their last closed flux-surfaces always remain in contact with the stationary limiter.

Assuming that the plasma moves vertically at an approximately *constant velocity*,[10] on a SOL/limiter resistive time scale, we can write

$$s = 1 - \hat{t}, \tag{41}$$

where $\hat{t}$ represents time normalized to this time scale. Thus, $\hat{t}=0$ corresponds to the start of the VDE (when the plasma first contacts the limiter), and $\hat{t}=1$ to the end (when the volume of the high-β plasma has shrunk to zero).

The halo thickness parameter, δ_h, is assumed to initially grow in proportion to the penetration of the plasma into the limiter (in such a manner that the total volume of the central high-β plasma and the low-β halo remains fixed). (Recall that the maximum radial width of the halo is $a\,\delta_h$.) However, it is also assumed that there is a maximum possible value that δ_h can take (determined, for instance, by the thickness of the limiter). This maximum value is denoted δ_{h0}. Thus, the halo thickness parameter is given by

$$\delta_h = \min(\hat{t}, \delta_{h0}). \tag{42}$$

Finally, it is assumed that the halo initially forms at constant plasma thermal energy density, i.e., constant $\hat{\beta}$, and constant toroidal plasma current, $\hat{I}_{p\phi}$, but that both these quantities are eventually quenched (as a consequence, for instance, of a sudden influx of impurities). Experimentally, it is generally found that the thermal quench takes place much more rapidly than the current quench.[10] The thermal and current quenches are crudely simulated in our model by linearly ramping the parameters $\hat{\beta}$ and $\hat{I}_{p\phi}$ from their initial values—$\hat{\beta}_0$ and $\hat{I}_{p\phi 0}$, respectively—to zero. The start of the thermal and current quenches is at $\hat{t}=\hat{t}_0$. The end of the thermal quench is at $\hat{t}=\hat{t}_1$, and the end of the current quench at $\hat{t}=\hat{t}_2$. The model is now completely specified.

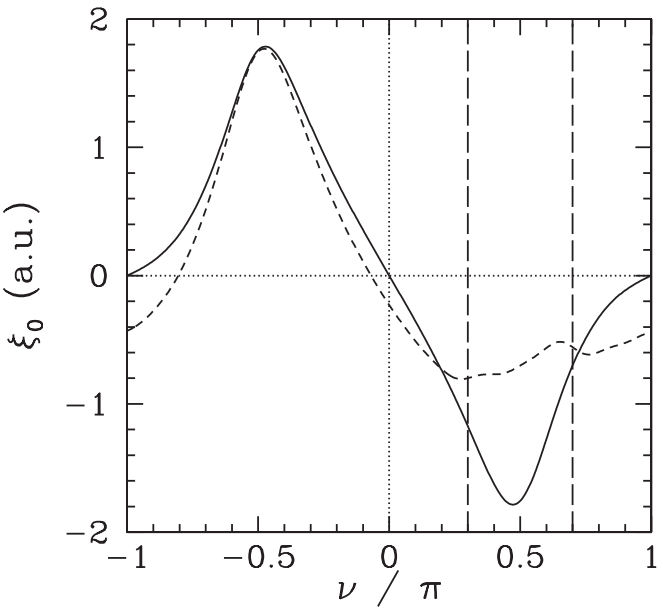

FIG. 2. The $n=0$ plasma displacement at the last closed flux-surface as a function of poloidal angle for a plasma equilibrium characterized by $\hat{\beta}=0.20$, $q_a=3.0$, $\kappa=2.0$, $s=1.0$, and $\delta_h=0.1$. The solid curve shows the displacement in the absence of a limiter force, whereas the dashed curve shows the displacement in the presence of a limiter force which is such as to render the $n=0$ mode marginally stable. The limiter lies between the two vertical dashed lines.

VII. EXAMPLE AXISYMMETRIC VDE SIMULATIONS

In the following, the limiter is assumed to lie above the plasma, and to extend from $\nu_1=0.3\pi$ to $\nu_2=0.7\pi$.

As a basic illustration of our method for determining the limiter force, consider a plasma equilibrium characterized by $\hat{\beta}=0.20$, $q_a=3.0$, $\kappa=2.0$, and $s=1.0$. Suppose that $\delta_h=0.1$. In the absence of a limiter force (i.e., $\hat{P}_0=0$), a calculation of the $n=0$ force-matrix yields one negative eigenvalue, $\lambda=-1.948\times10^{-1}$, indicating that the plasma is ideally unstable to the $n=0$ mode. However, if the limiter force parameter is adjusted such that $\hat{P}_0=4.075\times10^{-2}$, and the force-matrix is recalculated, then the negative eigenvalue is increased to zero (and all the other eigenvalues remain positive). (In general, there is only one value of $\hat{P}_0$ which can achieve this.) This indicates that the plasma can be rendered marginally stable to the $n=0$ mode by an axisymmetric halo current which arranges itself in such a manner that a normalized outward force per unit area of 4.075×10^{-2} is exerted on the limiter. Figure 2 shows the $n=0$ plasma displacement at the last closed flux-surface calculated in the absence, and in

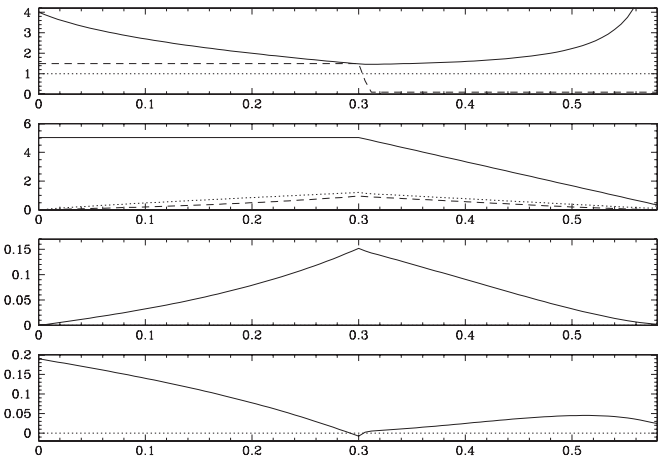

FIG. 3. Axisymmetric VDE simulation performed with $\kappa=2.0$, $\hat{\beta}_0=0.15$, $\hat{I}_{\phi 0}=5.04$, $\delta_{h0}=0.3$, $\hat{t}_0=0.30$, $\hat{t}_1=0.31$, and $\hat{t}_2=0.60$. The first panel shows q_a (solid curve) and $10\hat{\beta}$ (dashed curve) as functions of $\hat{t}$. The second panel shows $\hat{I}_{p\phi}$ (solid curve), $\hat{I}_{h\phi}$ (dotted curve), and $\hat{I}_{h\nu}$ (dashed curve). The third panel shows $\hat{P}_0$. Finally, the fourth panel shows the most negative eigenvalue of the $n=1$ F-matrix.

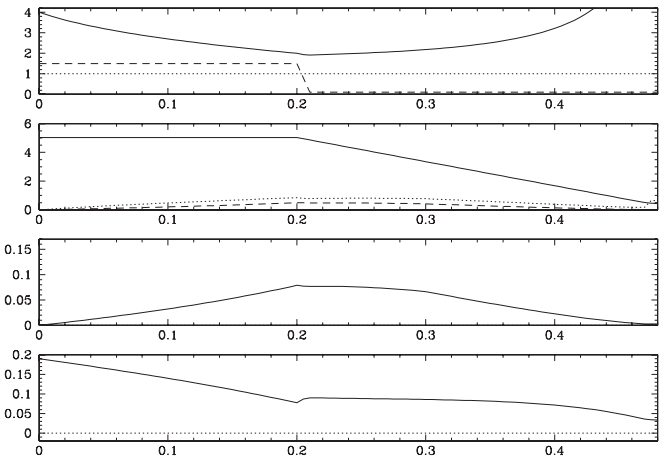

FIG. 4. Axisymmetric VDE simulation performed with $\kappa=2.0$, $\hat{\beta}_0=0.15$, $\hat{I}_{\phi 0}=5.04$, $\delta_{h0}=0.3$, $\hat{t}_0=0.20$, $\hat{t}_1=0.21$, and $\hat{t}_2=0.50$. The first panel shows q_a (solid curve) and $10\hat{\beta}$ (dashed curve) as functions of $\hat{t}$. The second panel shows $\hat{I}_{p\phi}$ (solid curve), $\hat{I}_{h\phi}$ (dotted curve), and $\hat{I}_{h\nu}$ (dashed curve). The third panel shows $\hat{P}_0$. Finally, the fourth panel shows the most negative eigenvalue of the $n=1$ F-matrix.

the presence, of the limiter force. The figure confirms that the $n=0$ mode is indeed a vertical instability. Moreover, it can be seen that, in the marginally stable case, the displacement is *locally reduced* in the limiter region, presumably as a consequence of the reaction force exerted on the plasma. Note that, as long as the instability grows on a resistive time scale, the displacement does not have to be zero in the limiter region. Indeed, a nonzero displacement indicates the diffusion of plasma magnetic flux-surfaces into the limiter.

Figure 3 shows an example axisymmetric VDE simulation performed using the following parameters: $\kappa=2.0$, $\hat{\beta}_0=0.15$, $\hat{I}_{p\phi 0}=5.04$ (corresponding to an initial edge-q of 4.0), $\delta_{h0}=0.3$, $\hat{t}_0=0.30$, $\hat{t}_1=0.31$, and $\hat{t}_2=0.60$. It can be seen that, as time progresses, and the high-β plasma gradually shrinks in size due to its interaction with the limiter, the edge safety-factor, q_a (which actually represents the safety-factor at the last closed flux-surface) initially *decreases*. This is a natural consequence of the shrinkage of the high-β plasma at constant toroidal plasma current.[10] The fall in the edge-q continues until the start of the current quench. During the current quench, the reduction in the plasma current is sufficiently rapid to offset the shrinkage of the high-β plasma, and the edge-q gradually *increases*, eventually becoming very large as the plasma current decays to zero. The toroidal and poloidal halo currents can be seen to rise as the edge-q decreases, and fall as it increases, and thus attain their peak values at the start of the current quench. Note that the peak toroidal and poloidal halo currents are about 20% of the initial toroidal plasma current. The limiter force can be seen to rise and fall in proportion to the poloidal halo current, and thus attains its peak value at the start of the current quench. This implies that the limiter force needed to make the $n=0$ mode marginally stable generally increases as the edge-q decreases. Finally, it can be seen that the most negative eigenvalue of the $n=1$ force-matrix is initially positive, indicating that the plasma is initially stable to the ideal $n=1$ kink mode. However, the eigenvalue decreases as the edge-q falls, and eventually becomes negative, indicating kink mode instability. Now, in the presence of an unstable kink mode, we expect the halo current to develop an $n=1$ component (see Sec. IX), which invalidates one of the central assumptions of our analysis (i.e., that the halo current is axisymmetric). Fortunately, the period of instability is comparatively brief, and is terminated by the onset of the thermal and current quenches.

Figure 4 shows an example axisymmetric VDE simulation performed using the following parameters: $\kappa=2.0$, $\hat{\beta}_0=0.15$, $\hat{I}_{p\phi 0}=5.04$ (corresponding to an initial edge-q of 4.0), $\delta_{h0}=0.3$, $\hat{t}_0=0.20$, $\hat{t}_1=0.21$, and $\hat{t}_2=0.50$. This simulation is identical to that shown in Fig. 3, except that the thermal and current quenches commence somewhat earlier. It can be seen that the earlier quench onset prevents the edge-q from falling to as low a value as in the first simulation. Consequently, the maximum (poloidal) halo current and limiter force are significantly reduced. Moreover, the $n=1$ mode remains robustly stable during the simulation.

VIII. GROWTH-RATE OF THE VERTICAL INSTABILITY

In our model, it is assumed that the halo current force considerably slows down the growth of the vertical instability. Let us now estimate the moderated growth-rate of this mode.

We shall assume that the halo current is predominantly a consequence of the inductive electric field generated by the reduction in the toroidal magnetic flux linked by the halo loop, as it shrinks in size. Applying Faraday's law to a poloidal circuit of the halo, we obtain[10]

$$2\pi\sqrt{\kappa}aE_\nu \sim 2\gamma B_o \pi\kappa a^2, \tag{43}$$

where γ is the growth rate, and a is the mean minor radius of the halo. Now, the halo current is (for the most part) constrained to flow parallel to magnetic field lines. Hence, the

component of the inductive electric field available to drive the current is

$$E_{\parallel} \sim \frac{B_{\nu}}{B_o} E_{\nu} \sim \frac{\gamma B_o \kappa a^2}{q_a R}. \tag{44}$$

Here, $q_a \sim B_o \sqrt{\kappa} a / B_{\nu} R$ is the edge safety factor. It follows that the halo current density is

$$j_{\parallel} = \sigma_h E_{\parallel}, \tag{45}$$

where σ_h is the average electrical conductivity of the halo. Thus, the toroidal and poloidal halo currents are

$$I_{h\phi} \sim \frac{2\pi\gamma B_o \sigma_h \kappa^{3/2} a^4 \delta_h}{q_a R}, \tag{46}$$

$$I_{h\nu} \sim \frac{I_{h\phi}}{q_a}, \tag{47}$$

since $a\delta_h$ is the radial thickness of the halo. Note that $\delta_h \ll 1$ (i.e., the halo is relatively thin). After normalization, the currents take the form

$$\hat{I}_{h\phi} \sim 2\pi\gamma\mu_0 \sigma_h a^2 \delta_h \frac{\kappa^{3/2}}{q_a}, \tag{48}$$

and $\hat{I}_{h\nu} = \hat{I}_{h\phi}/q_a$. According to Eq. (19), the limiter force parameter becomes

$$\hat{P}_0 = \frac{\hat{I}_{h\nu}}{2\pi} \sim \gamma\mu_0 \sigma_h a^2 \delta_h \frac{\kappa^{3/2}}{q_a^2}. \tag{49}$$

Now, the stability theory of Sec. V implies that the vertical instability is rendered marginally stable when $\hat{P}_0/\delta_h \sim 1$ (since all the other parameters in the theory are order unity). Hence, the halo current moderated vertical instability grows on the time scale

$$\gamma^{-1} \sim \mu_0 \sigma_h a^2 \frac{\kappa^{3/2}}{q_a^2}. \tag{50}$$

This time scale is certainly much longer than an Alfvén time, as was assumed earlier. Thus, a mode growing on such a time scale is effectively marginally stable as far as ideal-MHD stability theory is concerned. The growth time is also longer, by a factor δ_h^{-1}, than the L/R time of the halo (see Ref. 10). This suggests that any inductive time delay in setting up the halo current is negligible. Finally, the VDE growth time is probably longer than the L/R time of the vacuum vessel (which is of order $\mu_0 \sigma_w a_w d_w$, where σ_w, a_w, and d_w are the vessel conductivity, minor radius, and radial thickness, respectively) unless the vessel is both thick and highly conducting. This last observation offers some justification for the neglect of vacuum vessel eddy currents in our analysis—at least in the latter stages of a VDE when the plasma has made contract with the limiter—since it implies that halo currents are more effective at moderating the growth of the ideal vertical instability than vessel eddy currents.

IX. NONAXISYMMETRIC HALO CURRENTS

As has already been mentioned, we expect the halo current to develop a *nonaxisymmetric* component as soon as the most negative eigenvalue of the $n=1$ force-matrix (calculated in the presence of an axisymmetric halo current which is such as to render the $n=0$ mode marginally stable) becomes negative. Now, a nonaxisymmetric halo current is associated with *toroidal peaking* of the limiter force. We can measure of the degree of toroidal peaking via a so-called *toroidal peaking factor*, which is defined as the ratio of the maximum to the mean limiter force. (Another, more conventional, definition of the toroidal peaking factor is the ratio of the maximum to the mean poloidal limiter halo current.) The design of the ITER vacuum vessel is extremely sensitive to the assumed magnitude of the toroidal peaking factor. Thus, it is of paramount importance to predict the value of this parameter. In the following, we outline how this goal can be achieved.

The current sheet density associated with an $n=1$ halo current has the following components:

$$i_{h\nu} = \frac{P_1}{B_o} b \cos[\Theta(\nu) - \phi], \tag{51}$$

$$i_{h\phi} = \frac{P_1}{B_{\nu}} b \cos[\Theta(\nu) - \phi] \tag{52}$$

in the SOL, and

$$i_{h\nu} = \frac{P_1}{B_o} b \cos[\Theta^*(\nu) - \phi], \tag{53}$$

$$i_{h\phi} = \frac{P_1}{B_{\nu}} b(1 - b^{-1}) \cos[\Theta^*(\nu) - \phi] \tag{54}$$

in the limiter. Here, P_1 is a constant, and

$$b = \frac{\Theta(\nu_2) - \Theta(\nu_1)}{2\pi(q_a - 1)}, \tag{55}$$

$$\Theta(\nu) = \int_0^{\nu} \frac{h_a(\nu')}{\hat{B}_{\nu}(\nu')} d\nu', \tag{56}$$

$$\Theta^*(\nu) = \Theta(\nu)(1 - b^{-1}) + b^{-1}\Theta(\nu_2). \tag{57}$$

The above expressions are obtained by requiring that the $n=1$ halo current flow along magnetic field-lines in the SOL, flow along the shortest path in the limiter, and conserve charge. It follows that, in the presence of $n=0$ and $n=1$ halo currents, the (radially integrated) limiter pressure takes the form

$$P_h = P_0 + P_1 \cos[\Theta^*(\nu) - \phi]. \tag{58}$$

Of course, P_h is zero throughout the SOL. The toroidal peaking factor for the halo current force is thus

$$\mathcal{T} = 1 + \frac{|P_1|}{|P_0|}. \tag{59}$$

(The toroidal peaking factor for the poloidal limiter halo current is $\mathcal{T}_{\nu} = 1 + b|P_1|/|P_0|$.)

Now, the $n=1$ component of the limiter force gives rise to *coupling* between modes whose toroidal mode numbers differ by unity. In the presence of such a force, a straightforward generalization of the analysis in Sec. V yields the following eigenvalue equation which governs the stability of the coupled $n=0$ and $n=1$ modes:

$$\begin{pmatrix} \mathbf{F}_0 & \hat{P}_1\mathbf{K} \\ \hat{P}_1\mathbf{K}^\dagger & \mathbf{F}_1 \end{pmatrix}\begin{pmatrix} \boldsymbol{\xi}_0 \\ \boldsymbol{\xi}_1 \end{pmatrix} = \lambda\begin{pmatrix} \boldsymbol{\xi}_0 \\ \boldsymbol{\xi}_1 \end{pmatrix}. \tag{60}$$

Here, $\mathbf{F}_0$ is the $n=0$ force matrix, $\mathbf{F}_1$ the $n=1$ force matrix, $\boldsymbol{\xi}_0$ the $n=0$ eigenfunction, $\boldsymbol{\xi}_1$ the $n=1$ eigenfunction, and $\hat{P}_1=\mu_0 P_1/(\epsilon B_o)^2$. Moreover, the coupling matrix, $\mathbf{K}$, has the components

$$K_{mm'} = \frac{s\kappa}{2\delta_h}\oint \frac{\zeta}{h_a}\exp[-\mathrm{i}\Theta^*(\nu)+\mathrm{i}(m'-m)\nu]\frac{d\nu}{2\pi}. \tag{61}$$

In the above, we have neglected the coupling of the $n=1$ mode to the $n=2$ mode, for the sake of simplicity.

Let $\boldsymbol{\xi}_0=\xi_0\hat{\boldsymbol{\xi}}_0$ and $\boldsymbol{\xi}_1=\xi_1\hat{\boldsymbol{\xi}}_1$, where $\hat{\boldsymbol{\xi}}_0^\dagger\hat{\boldsymbol{\xi}}_0=\hat{\boldsymbol{\xi}}_1^\dagger\hat{\boldsymbol{\xi}}_1=1$. Here, ξ_0 and ξ_1 are the mean amplitudes of the $n=0$ and $n=1$ modes, respectively. We can write

$$\mathbf{F}_0\hat{\boldsymbol{\xi}}_0 = \lambda_0(\hat{P}_0)\hat{\boldsymbol{\xi}}_0, \tag{62}$$

$$\mathbf{F}_1\hat{\boldsymbol{\xi}}_1 = \lambda_1(\hat{P}_0)\hat{\boldsymbol{\xi}}_1, \tag{63}$$

and

$$\mathbf{K}\hat{\boldsymbol{\xi}}_1 = c\hat{\boldsymbol{\xi}}_0, \tag{64}$$

where

$$c = \hat{\boldsymbol{\xi}}_0^\dagger\mathbf{K}\hat{\boldsymbol{\xi}}_1. \tag{65}$$

Here, $\hat{\boldsymbol{\xi}}_0$ and $\hat{\boldsymbol{\xi}}_1$ represent the normalized eigenfunctions of the $n=0$ and $n=1$ force matrices, respectively. The corresponding eigenvalues (which are assumed to be the most negative ones) are λ_0 and λ_1. Of course, both these eigenvalues are functions of the axisymmetric halo current force parameter, $\hat{P}_0$. Here, for the sake of simplicity, we have neglected any change in shape of the $n=0$ and $n=1$ eigenfunctions due to the coupling produced by the nonaxisymmetric halo current.

Equation (60) reduces to

$$\begin{pmatrix} \lambda_0-\lambda & \hat{P}_1 c \\ \hat{P}_1 c^* & \lambda_1-\lambda \end{pmatrix}\begin{pmatrix} \xi_0 \\ \xi_1 \end{pmatrix} = \mathbf{0}. \tag{66}$$

This expression describes how the nonaxisymmetric halo current couples the $n=0$ and $n=1$ modes to produce two hybrid $n=0/n=1$ modes. The condition for one of these modes to be marginally stable is

$$\lambda_0\lambda_1 = \hat{P}_1^2|c|^2. \tag{67}$$

The eigenvalue of the other mode is then

$$\lambda = \lambda_0+\lambda_1. \tag{68}$$

Now, for the marginally stable mode

$$\frac{|\xi_1|}{|\xi_0|} = \frac{|\lambda_0|}{\hat{P}_1|c|}. \tag{69}$$

However, it is reasonable to suppose that the $n=1$ and $n=0$ limiter forces are in approximately the same ratio as the corresponding displacements, i.e.,

$$\frac{\hat{P}_1}{\hat{P}_0} \simeq \frac{|\xi_1|}{|\xi_0|}, \tag{70}$$

which leads to

$$\left(\frac{\hat{P}_1}{\hat{P}_0}\right)^2 \simeq \frac{|\lambda_0|}{\hat{P}_0|c|}. \tag{71}$$

Finally, we expect the limiter force to be a *positive definite* quantity. In other words, the plasma is able to push outward on the limiter, but not to pull inward, since, in the latter case, the plasma would instead lose contact with the limiter. In our simple model, in which the limiter force only has an $n=0$ and an $n=1$ component, this restriction implies that

$$\hat{P}_1 \leqslant \hat{P}_0, \tag{72}$$

i.e., the toroidal peaking factor for the halo current force cannot exceed 2, see Eq. (59). We can incorporate the restriction into Eq. (71) by writing

$$\left(\frac{\hat{P}_1}{\hat{P}_0}\right)^2 = \frac{|\lambda_0|}{\hat{P}_0|c|+|\lambda_0|}. \tag{73}$$

The solution to the problem is obtained by searching for a solution of Eqs. (67) and (73) for which the eigenvalue (68) is positive. This implies that the halo current renders one of the hybrid modes marginally stable, and the other stable. Of course, the marginally stable mode actually grows on a resistive time scale.

Note that we have made no attempt to find a rigorous solution of the $n=0/n=1$ eigenvalue equation (60). The reason for this is that our analysis does not take into account the fact that a slowly growing hybrid $n=0/n=1$ mode eventually makes the plasma equilibrium *three-dimensional*. Previously, this was not a problem, because a slowly growing pure $n=0$ mode converts an axisymmetric plasma equilibrium into another axisymmetric equilibrium. It follows that the above analysis is somewhat heuristic, since an accurate treatment of a nonaxisymmetric halo current would require force-matrix calculations made using kink-distorted plasma equilibria.

Figure 5 shows an example nonaxisymmetric VDE simulation. The simulation parameters are $\kappa=2.0$, $\hat{\beta}_0=0.15$, $\hat{I}_{p\phi 0}=5.04$ (corresponding to an initial edge-q of 4.0), $\delta_{h0}=0.3$, $\hat{t}_0=0.30$, $\hat{t}_1=0.31$, and $\hat{t}_2=0.60$. Of course, these

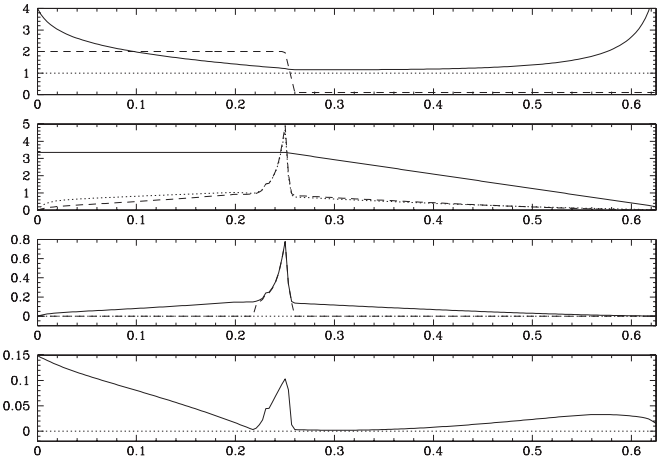

FIG. 5. Nonaxisymmetric VDE simulation performed with $\kappa=2.0$, $\hat{\beta}_0=0.15$, $\hat{I}_{\phi 0}=5.04$, $\delta_{h0}=0.3$, $\hat{t}_0=0.30$, $\hat{t}_1=0.31$, and $\hat{t}_2=0.60$. The first panel shows q_a (solid curve) and $10\hat{\beta}$ (dashed curve) as functions of $\hat{t}$. The second panel shows $\hat{I}_{p\phi}$ (solid curve), $\hat{I}_{h\phi}$ (dotted curve), and $\hat{I}_{h\nu}$ (dashed curve). The third panel shows $\hat{P}_0$ (solid curve) and $\hat{P}_1$ (dashed curve). Finally, the fourth panel shows the eigenvalue of the most unstable $n=1$ or hybrid $n=0/n=1$ mode, excluding the marginally stable mode.

parameters are the same as the those used in the axisymmetric VDE simulation shown in Fig. 3. It can be seen that the nonaxisymmetric VDE simulation is very similar to the corresponding axisymmetric one, except in the time period during which the latter simulation indicates an unstable $n=1$ kink mode. According to Fig. 5, the unstable kink mode triggers an intense burst of both axisymmetric and nonaxisymmetric halo current, with an associated spike in the maximum halo current force exerted on the limiter. Note that the toroidal peaking factor for the halo current force (i.e., $1+\hat{P}_0/\hat{P}_1$) quickly attains its maximum allowed value of 2 during the period of $n=1$ instability. The simulation suggests that the onset of kink instability during a VDE can give rise to a dangerous increase in the halo current force.

X. SUMMARY AND DISCUSSION

We have developed a simple model of axisymmetric vertical disruption events in tokamaks in which the halo current force exerted on the vacuum vessel (or whatever rigid conductor limits the plasma) is calculated *directly* from linear, marginally stable, ideal-MHD stability analysis. The basic premise of our model is that the halo current force modifies pressure balance at the edge of the plasma, and therefore also modifies ideal-MHD plasma stability. In order to prevent the ideal vertical instability, responsible for the VDE, from growing on the very short Alfvén time scale, the halo current force must adjust itself such that the instability is rendered *marginally stable*. This allows the vertical instability to develop on a relatively long time scale determined by resistive diffusion of magnetic flux-surfaces through the scape-off layer and vacuum vessel, see Sec. VIII. Consequently, the plasma remains in an approximate *axisymmetric equilibrium state* throughout the duration of the VDE. This explains why it is valid to employ *linear* ideal-MHD to characterize the vertical stability of the plasma at each stage of the VDE.

We have used our model to perform a number of crude simulations of axisymmetric VDEs in tokamaks, see Sec. VII. These simulations predict halo currents and halo current forces which are similar in magnitude to those observed in experiments.[10] In addition, the simulations indicate that the halo current increases in magnitude as the edge-q decreases, and that an $n=1$ kink mode is triggered if the edge-q becomes too close to unity. These conclusions are also in broad agreement with experimental data.[10]

We have generalized our model to deal with a *nonaxisymmetric* halo current induced by the $n=1$ kink mode, see Sec. IX. This extended theory allows us to predict the peak halo current force exerted on the vacuum vessel. However, our nonaxisymmetric model requires some improvement in order to make it truly rigorous.

One important effect which is absent from our model is the moderating influence of eddy currents flowing in external conductors, such as, the vacuum vessel, on the vertical instability. Some justification for the omission of this effect in the latter stages of a VDE is given in Sec. VIII. For the sake of simplicity, we have also neglected any change in the plasma shape associated with the growth of the vertical mode. Finally, it has been assumed that the inductive electric fields generated by a VDE are sufficiently large to cause the breakdown of any sheaths at the plasma/limiter boundary, and, consequently, that the halo current magnitude is not limited by the ion polarization current.

ACKNOWLEDGMENTS

The author would like to thank L. Zahkarov (PPPL) for providing the crucial insight which made this paper possible.

This research was funded by the U.S. Department of Energy under Contract No. DE-FG05-96ER-54346.

[1] J. A. Wesson, R. D. Gill, M. Hugon, F. C. Schuller, J. A. Snipes, D. J. Ward, D. V. Bartlett, D. J. Campbell, P. A. Duperrex, A. W. Edwards, R. S. Granetz, N. A. O. Gottardi, T. C. Hender, E. Lazzaro, P. J. Lomas, N. L. Cardozo, K. F. Mast, M. F. F. Nave, N. A. Salmon, P. Smeulders, P. R. Thomas, B. J. D. Tubbing, M. F. Turner, and A. Weller, Nucl. Fusion **29**, 641 (1989).

[2] E. J. Strait, L. L. Lao, J. L. Luxon, and E. E. Reis, Nucl. Fusion **31**, 527 (1991).

[3] K. Ioki, G. Johnson, K. Shimizu, and D. Williamson, Fusion Eng. Des. **27**, 39 (1995).

[4] S. Mirnov, J. Wesley, N. Fujisawa, Yu. Gribov, O. Gruber, T. Hender, N. Ivanov, S. Jardin, J. Lister, F. Perkins, M. Rosenbluth, N. Sauthoff, T. Taylor, S. Tokuda, K. Yamazaki, R. Yoshino, A. Bondeson, J. Conner, E. Fredrickson, D. Gates, R. Granetz, R. La Haye, J. Neuhauser, F. Porcelli, D. E. Post, N. A. Uckan, M. Azumi, D. J. Campbell, M. Wakatani, W. M. Nevins, M. Shimada, and J. Van Dam, Nucl. Fusion **39**, 2251 (1999).

[5] T. C. Hender, J. C. Wesley, J. Bialek, A. Bondeson, A. H. Boozer, R. J. Buttery, A. Garofalo, T. P. Goodman, R. S. Granetz, Y. Gribov, O. Gruber, M. Gryaznevich, G. Giruzzi, S. Günter, N. Hayashi, P. Helander, C. C. Hegna, D. F. Howell, D. A. Humphreys, G. T. A. Huysmans, A. W. Hyatt, A. Isayama, S. C. Jardin, Y. Kawano, A. Kellman, C. Kessel, H. R. Koslowski, R. J. La Haye, E. Lazzaro, Y. Q. Liu, V. Lukash, J. Manickam, S. Medvedev, V. Mertens, S. V. Mirnov, Y. Nakamura, G. Navratil, M. Okabayashi, T. Ozeki, R. Paccagnella, G. Pautasso, F. Porcelli, V. D. Pustovitov, V. Riccardo, M. Sato, O. Sauter, M. J. Schaffer, M. Shimada, P. Sonato, E. J. Strait, M. Sugihara, M. Takechi, A. D. Turnbull, E. Westerhof, D. G. Whyte, R. Yoshino, H. Zohm, and the ITPA MHD, Disruption, and Magnetic Control Topical Group, Nucl. Fusion **47**, S128 (2007).

[6] T. H. Jensen and D. G. Skinner, Phys. Fluids B **2**, 2358 (1990).

[7] J. P. Freidberg and F. Haas, Phys. Fluids **17**, 440 (1974).

[8]R. Fitzpatrick, Phys. Plasmas **15**, 092502 (2008).
[9]F. Hofmann, M. J. Dutch, D. J. Ward, M. Anton, I. Furno, J. B. Lister, and J.-M. Moret, Nucl. Fusion **37**, 681 (1997).
[10]D. A. Humphreys and A. G. Kellman, Phys. Plasmas **6**, 2742 (1999).
[11]R. Fitzpatrick, Phys. Plasmas **14**, 062505 (2007).
[12]J. P. Freidberg, *Ideal Magnetohydrodynamics* (Springer, Berlin, 1987).
[13]L. E. Zakharov, Phys. Plasmas **15**, 062507 (2008).
[14]V. Riccardo, T. C. Hender, P. J. Lomas, B. Alper, T. Bolzonella, P. de Vries, G. P. Maddison, and the JET EFDA Contributers, Plasma Phys. Controlled Fusion **46**, 925 (2004).